Mol Cell Toxicol (2015) 11:19-28
DOI 10.1007/s13273-015-0003-9

ORIGINAL PAPER

MicroRNA expression profiling of *p*-phenylenediamine treatment in human keratinocyte cell line

Hwa Jun Cha[1], Ok-Kyu Lee[1], Soo Yeon Kim[1], Jung-Min Ko[1], Su Young Kim[1], Ji Hye Son[1], Hyun Joo Han[1], Shunhua Li[2], Soo Young Kim[3], Kyu Joong Ahn[3], In-Sook An[1], Sungkwan An[1] & Seunghee Bae[1]

Received: 17 September 2014 / Accepted: 20 November 2014

Abstract *p*-Phenylenediamine (PPD), a black dye used in hair coloring and tattoos, irritates the skin, leading to cell cycle arrest, apoptosis, and reactive oxygen species (ROS) generation. MicroRNAs (miRNAs) are well known regulators of these side effects. The aim of the present study was to evaluate PPD-induced miRNA expression profile alterations in human keratinocytes. First, we demonstrated that PPD reduced HaCaT cell viability by inducing cell cycle arrest and death, elevating cellular ROS levels and decreasing the migration rate. In addition, 67 miRNAs were upregulated by at least 5-fold in PPD-treated HaCaT cell and 17 miRNAs were downregulated by at least 5-fold in PPD-treated HaCaT cell. Using bioinformatics, we identified a relationship between PPD-mediated miRNA changes and cell death, cell cycle arrest, generation of ROS, and migration repression. Target genes of PPD-regulated miRNAs were involved in cell proliferation, apoptosis, skin development, and aging. Thus, our results establish a role for miRNAs in regulating PPD-induced cell death, cell cycle arrest, ROS generation, and repression of migration in human keratinocytes.

Keywords *p*-Phenylenediamine, Human keratinocytes, microRNA

[1]Korea Institute for Skin and Clinical Sciences and Molecular-Targeted Drug Research Center, Konkuk University, Seoul, Korea
[2]Department of Beauty Education, Graduate School of Education, Konkuk University, Seoul, Korea
[3]Department of Dermatology, Konkuk University School of Medicine, Seoul, Korea
Correspondence and requests for materials should be addressed to S. Bae (✉ sbae@konkuk.ac.kr)

The monocyclic arylamine *p*-phenylenediamine (PPD, also known as black henna), which is used in hair coloring and tattoos, is one of the most frequently used commercial oxidative-type dyes[1]. Under oxidative conditions, PPD reacts and polymerizes with hair-coloring molecules[2-4]; however, after hair coloring, less than 1% of the PPD remains bound[5]. PPD is responsible for skin irritation and allergic contact dermatitis. The molecular mechanism underlying PPD-mediated irritation and allergies has been revealed in previous studies[8,9] and involves the formation of immunogenic hapten-protein conjugates[6,7]. In addition, PPD damages DNA through various mechanisms, such as chromosomal aberrations, telomere dysfunction, cell cycle arrest, and apoptosis[10]. Finally, when PPD enters the body, it induces cytotoxicity via reactive oxygen species (ROS) formation, and the activation of p38 and JNK in the liver[11]. MicroRNAs (miRNA) are 20-22 nucleotide noncoding RNAs that play a crucial role in post-transcriptional modification by binding the 3′ untranslated terminal region (3`UTR) of target genes[12]. Various toxicants, such as a PPARα agonist, ethanol, cigarette smoke, etc., have been identified as inducing a toxic response in miRNAs through the alteration of miRNA expression. Significantly, PPD-induced skin irritation is accompanied by apoptosis, cell cycle arrest, and ROS generation[13-15]. Interestingly, many miRNAs have documented roles in apoptosis, cell cycle arrest, and ROS generation[16-18]. For example, the miR-99a and -16 families are overexpressed in cell cycle arrest, regulating the cell cycle by targeting the key molecules mammalian target of rapamycin (mTOR) and cyclin D1[19,20]. miR-15 and miR-16 target B-cell lymphoma 2 (BCL2) in apoptosis[21]. As well, miR-21 modulates ROS levels by

directly targeting superoxide dismutase 3 (SOD3)[22]. miRNA expression is altered by exposure to various environmental toxic compounds[23]. Thus, the bulk of evidence implicates miRNAs in PPD irritation, a cellular response induced by a toxic compound. In addition, the miRNAs is regulated by general exogenous toxicants such as environmental stressors, toxins, drugs and chemicals[24]. Representative examples of miRNAs implicated in cellular response of toxicants are Let-7c, miR-294, miR-34c, miR-222 and miR-218 which are regulated by cigarette smoke[24]. In this study, we characterized miRNA expression in PPD-treated human keratinocyte HaCaT cells using miRNA microarrays. Our expression profiling provides potential miRNA-based biomarkers for PPD-induced side effects, as well as evidence concerning PPD's mechanism of action in human keratinocytes.

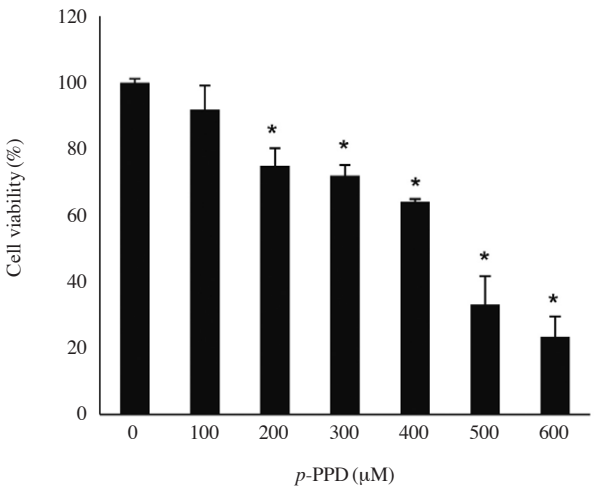

Figure 1. PPD-induced cytotoxicity in HaCaT cells. HaCaT cells (1×10^4) were incubated with PPD at the indicated concentrations (0-600 μM) for 24 h. After incubation, cytotoxicity was measured using WST-1. Formazan concentration was analyzed by measuring optical density at 405 nm. Data are presented as mean ± standard deviations from three experiments. *$P < 0.05$.

Results & Discussion

Effects of PPD on HaCaT viability and the cell cycle

PPD concentration (0-600 μM)-dependent HaCaT viability was analyzed via the WST-1 assay (Figure 1). Treatment with concentrations ≥ 100 μM reduced cell viability after 24 h in a dose-dependent manner. At doses > 500 μM, PPD-treated cells were less than 50% viable compared to non-treated cells. Our next experiments employed 400 μM PPD. As shown in Figure 2A, B, PPD increased the sub-G1 cell population, indicating cell death. In addition, the G1/G2 ratio decreased, indicating the induction of G2 arrest (Figure 2A, C). Therefore, we suggest that the PPD-induced decrease in viability results from cell death and G2 arrest.

Effects of PPD on intercellular ROS levels

PPD is widely known to cause ROS-induced cell death and to arrest growth in a wide range of cell lines, such as liver cells, neutrophils, and kidney cells[11,25,26]. We assessed the question of whether PPD was able to induce ROS in keratinocytes. Cytometrical analysis revealed that PPD leads to a high percentage of M gate cells, indicating elevated intercellular ROS levels (Figure 3A, B).

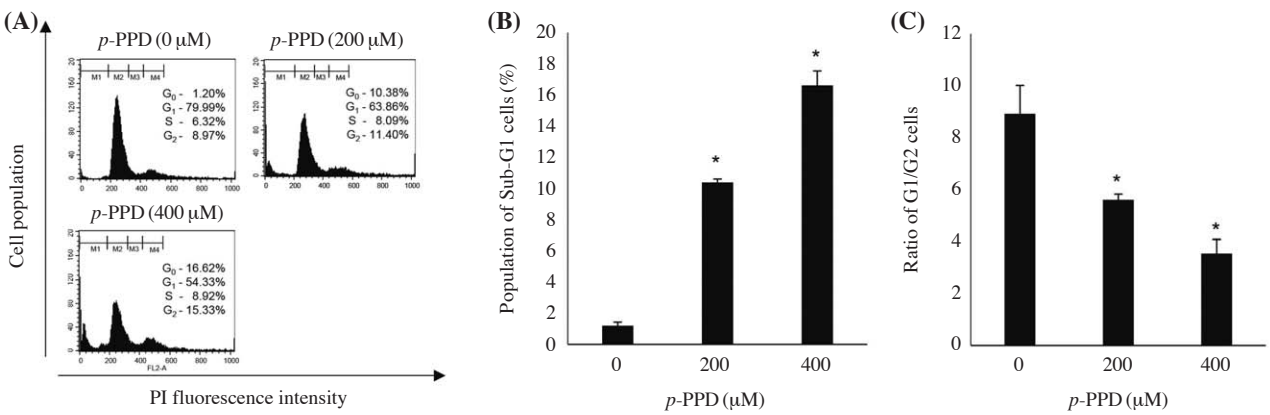

Figure 2. PPD induces cell cycle arrest and cell death in nHDPCs. HaCaT cells (5×10^5) were incubated with PPD at the indicated concentrations (0, 200, and 400 μM) for 24 h. After incubation, nHDPCs were collected, stained with PI, and analyzed using a flow cytometer. PI-stained cells were analyzed by measuring the intensity of the FL2 channel. Data are presented as (A) histogram plots, and (B-C) bar graphs of the percentage of gates (M1-sub-G1, M2-G1, M3-S, and M4-G2). (B) Proportion of sub-G1 cells; (C) G1/G2 cell ratio. *$P < 0.05$.

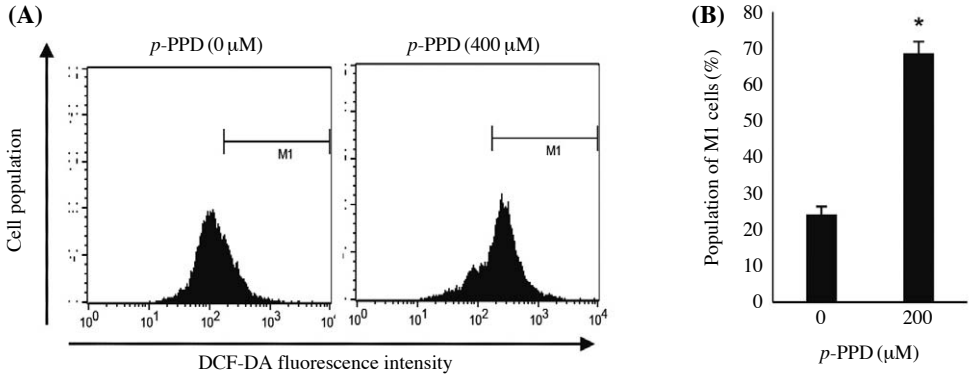

Figure 3. PPD-induced intercellular ROS in HaCaT cells. Flow-cytometric analysis of ROS levels. HaCaT cells (5×10^5) were incubated with PPD at the indicated concentrations (0, 200, and 400 μM) for 24 h. After incubation, cells were collected, DCF-stained, and analyzed using a flow cytometer. DCF-stained cells were analyzed by measuring the intensity of the FL1 channel. Data are presented as (A) histogram plots and (B) a bar graph of the percentage of M1 cells. $*P < 0.05$.

Effects of PPD on cell migration

Next, we examined whether PPD reduces migration in HaCaT cells. Treatment with 400 μM PPD decreased migration relative to non-treated cells (Figure 4). Thus, PPD reduced migration in HaCaT cells.

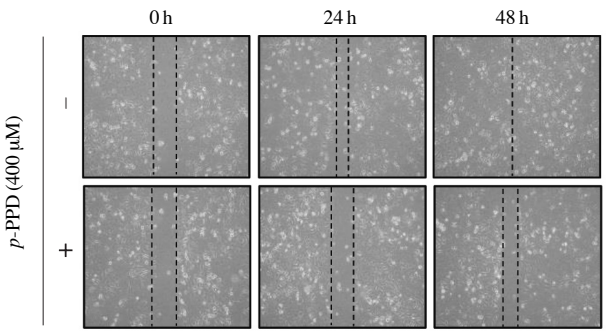

Figure 4. PPD-induced migration in HaCaT cells. Migration was analyzed using a scratch-based migration assay. HaCaT cells (5×10^5) were incubated until confluent, then a scratch-based migration assay was performed. After scratch, cells were incubated with PPD for 0, 24, or 48 h, and then photos of cells were taken using a microscope at the indicated time.

Effect of PPD on miRNA expression profile

In this study, we showed that treatment with 400 μM PPD reduced viability and migration and increased intercellular ROS levels, cell death, and G2 arrest in HaCaT cells. To investigate whether PPD also altered the miRNA expression profile at 400 μM, we performed miRNA microarray analysis on PPD-treated cells and controls (Figure 5). A total of 84 miRNAs (upregulated 67 miRNAs and downregulated 17 miRNAs) changed at least 5-fold in PPD-treated cells, as shown in Table S1. miR-1471 showed the greatest increase in expression relative to the control cells (375.0-fold), whereas miR-221-5p showed the greatest decrease (-362.5-fold). These results implicate miRNA expression changes in the PPD-induced cellular response. Therefore, we identified the targets of PPD up- and downregulated miRNAs using DIANA, a seed sequence-based miRNA target prediction program. To extract the biological significance of the targets, we categorized them according to four functions: aging, skin development, apoptosis, and cell proliferation-related gene ontology (GO) (Tables S2, S3). The categorized terms contained bi-directional processes for each term. For example, 'Aging' included both aging and anti-aging processes. Therefore, we analyzed that a high number of target genes of up- and down-regulated miRNAs was associated with four categorized groups (aging, skin development, apoptosis, and cell proliferation). Actually, of those, some miRNAs, miR494 and miR708-5p, were well-identified in terms of their functions and targets in a previous study. miR-494, which was upregulated 6.7-fold in our study, has been reported to suppress cell proliferation and induce senescence by targeting insulin-like growth factor 2 mRNA-binding protein 1 (IGF2BP1)[27,28]. miR-708-5p, upregulated 16.2-fold in our study, has been reported to induce apoptosis by targeting surviving[29]. Next, we identified meaningful KEGG pathways regulated by genes targeted by PPD-induced miRNAs (Tables S4, S5). Target genes of the top 15 miRNAs which were up- and down-regulated by PPD were associated with various KEGG pathways. Of those, "MAPK signaling", which regulates apoptosis and proliferation in various conditions[30,31], was related to the targets of miR-7-1-3p, 493-3p, 28-5p, and 9-5p, which is significantly regulated by PPD. Interestingly, in a previous study, PPD was shown to induce apoptosis through activation of the MAPK signaling pathway molecules JNK and p38[11]. In addition, when these KEGG pathways which

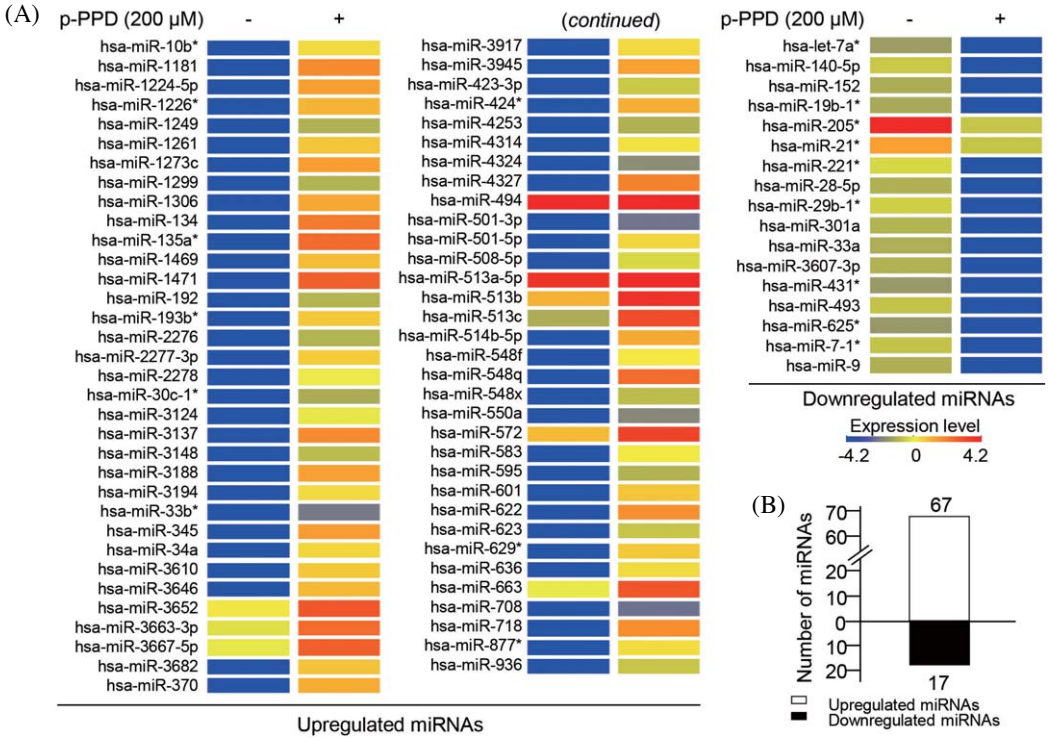

Figure 5. PPD is associated with changes in the miRNA expression profile. (A) Heat-map of 5-fold upregulated and downregulated miRNAs in cells treated with PPD vs. controls. (B) Graph showing the number of dysregulated miRNAs.

were associated with target genes of PPD-mediated miRNAs regulated by PPD were compared with the findings of Ryu *et al.*[8], we found that regulation of "p53 signaling" related to the targets of miR-152, 301a-3p and "cell cycle" related to the targets of miR-152, 301a-3p were implicated in PPD-induced cell death and cell cycle arrest. Actually, PPD induces cell death and cell cycle arrest through the activation of p53[25]. Overall, the present study provides evidence of the toxic effects of PPD in HaCaT cells. In addition, we have demonstrated that PPD induced the alteration of the miRNA expression profile, which can regulate viability, cell cycle, ROS generation, migration through targeting aging, skin development, proliferation and apoptosis related genes.

Materials & Methods

Cell culture and materials

The human keratinocyte HaCaT cell line was cultured in EpiLife® medium (Life Technologies Gibco, Grand Island, NY, USA) supplemented with human keratinocyte growth supplement (HKGS; Life Technologies Gibco), penicillin, and streptomycin (Life Technologies Gibco). HaCaT cells were maintained under standard culture conditions at a temperature of 37°C and an atmosphere of 5% CO_2. Cells were subcultured twice a week. PPD was purchased from Sigma-Aldrich (St. Louis, MO, USA), and stock solutions were prepared in dimethyl sulphoxide (DMSO; Sigma-Aldrich) and administered at the concentration indicated. The maximum final concentration of DMSO was limited to 0.1% (v/v) of medium.

Analysis of cell viability

Cytotoxicity and effects on cell growth were assessed using Cell Proliferation Reagent WST-1 (EZ-Cytox Cell Viability Assay Kit; Itsbio, Seoul, Korea). Briefly, 1×10^4 HaCaT cells were seeded in a 96-well plate. After 24 h incubation, the indicated concentrations of PPD were administered and cells were incubated for 24 h. Then, Cell Proliferation Reagent WST-1 was added to each well and incubated for 30 min. Absorbance was measured at 490 nm with a microplate reader (iMark, Bio-Rad, Hercules, CA, USA).

Analysis of cell cycle

Cell cycle populations were determined in a propidium iodide (PI)-based analysis. First, 5×10^5 HaCaT cells

Table S1. miRNAs showing >5-fold changes in expression in HaCaT cells following treatment with PPD.

miRNA (*Homo sapiens*)	F.C.[a]	Chr.[b]	miRNA (*Homo sapiens*)	F.C.	Chr.	miRNA (*Homo sapiens*)	F.C.	Chr.
miR-10b-3p	76.0	chr2	miR-3646	111.7	chr20	miR-595	32.8	chr7
miR-1181	200.4	chr19	miR-3652	6.2	chr12	miR-601	96.4	chr9
miR-1224-5p	153.4	chr3	miR-3663-3p	6.3	chr10	miR-622	188.7	chr13
miR-1226-5p	117.2	chr3	miR-3667-5p	6.7	chr22	miR-623	39.7	chr13
miR-1249	32.1	chr22	miR-3682-3p	100.2	chr2	miR-629-3p	92.9	chr15
miR-1261	96.0	chr11	miR-370	131.1	chr14	miR-636	75.9	chr17
miR-1273c	155.3	chr6	miR-3917	76.7	chr1	miR-663a	7.6	chr20
miR-1299	32.9	chr9	miR-3945	150.0	chr4	miR-708-5p	16.2	chr11
miR-1306	137.0	chr22	miR-423-3p	40.5	chr17	miR-718	195.4	chrX
miR-134	262.9	chr14	miR-424-3p	126.0	chrX	miR-877-3p	74.0	chr6
miR-135a-3p	318.5	chr3	miR-4253	32.0	chr1	miR-936	39.5	chr10
miR-1469	106.5	chr15	miR-4314	70.7	chr17	let-7a-3p	−71.8	chr9
miR-1471	375.0	chr2	miR-4324	21.9	chr19	140-5p	−246.6	chr16
miR-192-5p	33.4	chr11	miR-4327	231.0	chr21	miR-152	−115.3	chr17
miR-193b-5p	94.2	chr16	miR-494	6.7	chr14	miR-19b-1-5p	−104.2	chr13
miR-2276	33.0	chr13	miR-501-3p	16.7	chrX	205-3p	−15.3	chr1
miR-2277-3p	88.5	chr5	miR-501-5p	80.6	chrX	miR-21-3p	−5.0	chr17
miR-2278	57.8	chr9	miR-508-5p	46.95	chrX	miR-221-5p	−362.5	chrX
miR-30c-1-3p	30.7	chr1	miR-513a-5p	5.9	chrX	miR-28-5p	−127.5	chr3
miR-3124-5p	54.6	chr1	miR-513b	6.4	chrX	miR-29b-1-5p	−293.5	chr7
miR-3137	209.1	chr3	miR-513c	16.4	chrX	miR-301a-3p	−135.8	chr17
miR-3148	36.0	chr8	miR-514b-5p	135.6	chrX	miR-33a-5p	−116.3	chr22
miR-3188	147.0	chr19	miR-548f	67.0	chr2	miR-3607-3p	−133.4	chr5
miR-3194-5p	75.8	chr20	miR-548q	320.9	chr10	431-3p	−63.1	chr14
miR-33b-3p	17.7	chr17	miR-548x	36.4	chr21	493-3p	−215.3	chr14
miR-345-5p	161.4	chr14	miR-550a-5p	20.5	chr7	miR-625-3p	−60.0	chr14
miR-34a-5p	79.2	chr1	miR-572	5.2	chr4	miR-7-1-3p	−218.2	chr9
miR-3610	93.3	chr8	miR-583	66.9	chr5	miR-9-5p	−122.2	chr1

[a]F.C., fold change; [b]Chr, chromosome

were seeded in a 6-well plate and treated with PPD. Cells were harvested 24 h later, fixed in 70% ethanol, and stained with PI (50 μg/mL PI, RNase 0.1 μg/mL, and 0.05% Triton X-100 in PBS). Cytometrical analysis was conducted with a FACSCaliber flow cytometer (BD Biosciences, San Jose, CA, USA), and 1×10^4 cells were counted in each group, each phase of the cell cycle population being determined by gate.

Analysis of intercellular ROS levels

Intercellular ROS levels were determined using a 2′,7′-dichlorofluorescin diacetate (DCF-DA)-based analysis. First, 5×10^5 HaCaT cells were seeded in a 6-well plate and treated with PPD. Cells were stained with 20 μM DCF-DA 24 h later. These cells were harvested and analyzed with a FACSCaliber flow cytometer (BD Biosciences, San Jose, CA, USA) to measure ROS levels, with 1×10^4 cells counted in each group.

Analysis of migration

Migration was determined using a scratch-based assay. First, 5×10^5 HaCaT cells were seeded in a 6-well plate and incubated in a monolayer to >90% confluence. Next, a 200 μL pipette tip was used to scratch the center of the well. After scratching, PPD treatments were administered and cells were incubated for 48 h. At 0, 24, and 48 h, photos of the scratched wells were taken with a microscope.

Analysis of miRNA expression profile

Total RNA was isolated with TRIZol® reagent according to the manufacturer's instructions. Concentration was determined by measuring absorbance at 260 nm with a MaestroNano (Maestrogen, Las Vegas, NV, USA). Total RNA was dephosphorylated and labeled with pCp-Cy3 using an Agilent miRNA labeling kit (Agilent Technologies, Santa Clara, CA, USA). Unlabeled RNAs were eliminated using a Micro Bio-Spin P-6 column (Bio-Rad Laboratories, Hercules, CA, USA), and labeled RNAs were hybridized to a Sure Print G3 Human v16 miRNA 8 × 60 K Microarray (Agilent Technologies) at 65°C for 20 h. The microarray was scanned using an Agilent microarray scanner (Agilent Technologies), and feature extraction software (Agilent Technologies) was used to digitize the data

Table S2. Predicted targets of top 15 PPD-upregulated miRNAs in HaCaT cells.

miRNA (*Homo sapiens*)	Target genes and functions			
	Aging	Skin development	Apoptosis	Cell proliferation
miR-1471	–	–	–	–
miR-548q	NOS3, DBH, SREBF2	–	NOS3, DBH, MED1, EYA1, FOXC1, MAPK7, APBB1, DDX41, BRAF, BNIP3L, BCAP29, TOAK1	NOS3, EYA1, FOXC1, GAS8, PRMT5, DBH, MED1, PDPN
miR-135a-3p	PTEN, FADS1	TFAP2A, COL8A1	PTEN, TFAP2A, LRP6, KRIT1, ESR1, DYNLL2, RRP8, PEG3, PSMB2, CKAP2, MST4	PTEN, TFAP2A, LRP6, ESR1, DERL2, RERG, COL8A1
miR-134	EDN1, CISD2	COL5A2	EDN1, BDNF, ITGB1, BARD1, STAT5B, CREB1, IKBKG, SLIT3, PAX8, PAWR, PDCD7	EDN1, BDNF, ITGB1, PAWR, STAT5B, MAGI2, TRIM27, KRAS, PKD2, CDK13
miR-4327	RPS6KBI	STS	RPS6KBI, ADAMT520, ATG5, IGF1R, FGD4, ROBO2	RPS6KBI, IGF1R, SOX2, NF2, FOSL2
miR-3137	HMGA2, CDK6	CTNNB1	HSPD1, FLT3, WNT11, DDX5, SENP1, TIA1, BRCA1, FAF1, HMGA2, CTNNB1, FGFR2, GDNF, RAG1, BARD1	HMGA2, CDK6, CTNNB1, BRCA1, FGFR2, WNT11, ERG, NFIB, FBXW7
miR-1181	–	–	–	–
miR-718	–	TFAP2A	TFAP2A, BAD, CTSH	TFAP2A, BAD, CTSH
miR-622	SIRT1, NPM1, BBC3, ID2, PTEN	TCF7L2, LEF1, COL2A1	RB1, DDX5, RASA1, PSMD1, SIRT1, NPM1, PTEN, BBC3, LEF1, NF1, EYA1, PPARD, COL2A1, PEA15, TRAF7	SIRT1, NPM1, PTEN, TCF7L2, LEF1, NF1, ID2, EYA1, TGIF, PPARD, RB1, MBD2
miR-345-5p	SLC1A2	–	MAPK1, IRF1, HDAC2, IP6K2	MAPK1, IRF1, HDAC2, TOB1
miR-1273c	PTH1R	–	MEF2C	PTH1R, MEF2C, FGF9
miR-1224-5p	HMGA2, SCL1A2, PLA2R1, AQP2	APC	HMGA2, AQP2, TIAF1, SLIT2, SATB1, APC, FGFR1, TAOK1, CREB1, E2F2, TRAF2, RIPK1, STAT5B	SATB1, FGFR1, NEUROD4, HMGA2, DERL2, STAT5B, DLG5, APC, ATF3
miR-3945	–	–	ESR1, BIRC6, ERCC3, PPT1, C1D, SORT1, BCL2L2	ESR1, BIRC6, FGF19, DLEC1
miR-3188	AGT, SLC1A2	DHCR24, COL5A1	KLF11, CLIP3, ATG5, VIM, AGT, DHCR24, MAGED1, HIPK1, RARG, HDAC2, RRN3, CYLD	AGT, DHCR24, MAGED1, HIPK1, RARG, HDAC2, KLF11, RRN3, SMAD2
miR-1306-3p	–	TFAP2A	TFAP2A	TFAP2A

from the scanned image. Fold change was calculated from digitized data using GeneSpring GX (Agilent Technologies).

Analysis of putative target genes and their functions

Targets of miRNAs with altered expression levels were analyzed using DIANA (http://diana.cslab.ece.ntua.gr/), which classifies genes into groups with similar functional patterns.

Statistical analysis

Statistical analysis was performed using the paired Student's t-test. Asterisks were used to indicate statistical significance ($P < 0.05$).

Acknowledgements This study was supported by the KU Research Professor Program of Konkuk University and a grant from the Korean Health Technology R&D Project (Grant No. HN13C0080), Ministry of Health & Welfare, Republic of Korea. HJ Cha, O-K Lee, SY Kim, J-M Ko,

Table S3. Predicted targets of top 15 PPD-downregulated miRNAs in HaCaT cells.

miRNA (*Homo sapiens*)	Target genes and functions			
	Aging	Skin development	Apoptosis	Cell proliferation
miR-221-5p	TP63, CASP2, HTT, LRP1, MAP2K1	TP63	TP63, CASP2, HTT, JAK2, ITGB1, VDAC1, PCSK9	TP63, MAP2K1, LRP1, JAK2, ITGB1, TXLNA, MST1R, IMPDH1
miR-29b-1-5p	SIRT1, NR3C1, TERF2	−	SIRT1, NR3C1, PTK2, FOXC1, HIPK1, REST, PSMD7, PERP, BNIP3L, WNK3, SOS2	SIRT1, NR3C1, PTK2, FOXC1, HIPK1, REST, TNC, CABBR1, FEZF2, SMARCD3, NFIB, INSR, FGF18, PRRX1
miR-140-5p	FADS1	−	EIF2AK2, SOX4, HAND2, BCL2L1, BMP2, BIRC6, ING3, PKN2, FXR1	BMP2, SOX4, BIRC6, IGFBP5, EIF2AK2, HAND2, BCL2L1, ADAM10, WNT9A, TACC1, EVI5, FGF9, UBR5
miR-7-1-3p	BCL2, SMC5, PTEN, CTGF, CDK6, LRP2, ATR, TIMP3, MARCH5, TGFBR1, SLC1A2	BCL11B, SHH, PDGFA, IRF6	BCL2, TGFBR1, PTEN, CTGF, SATB1, PAWR, SOX7, IGF1R, BDNF, HDAC2, EST1, MSX1, TRAF6, ROBO2, SKIL, SOS1, AR, HIPK1, DICER1, ERBB4, BCL11B, CDKN2C, COL4A3, NOTCH2, CADM1, BCLAF1, MAP3K1, SIAH1, MEF2D, TRAF7, HIPK3, BNIP2, GSK3B, SIX4	BCL2, TGFBR1, PTEN, CTGF, HIPK1, ERBB4, SATB1, IRF6, CDKN2C, DICER1, NOTCH2, MSX1, BDNF, TIAL1, PAWR, CDK6, LRP2, BCL11B, EST1, SOX7, IGF1R, EVIS, PDGFA, CD164, PELI1, E2F3, CDC42, COL4A3, HDAC2, CDKN2B, TGIF1, HOXA3, AR, TFDP1, RUNX1, CASK, FZD7, LIFR, EREG, DERL2, CDC27
miR-493-3p	PLA2R1, BBC3	SHH, GNAS, COL5A1, LTB	ETS1, VDAC1, RAC1, PARK2, BBC3, AKT2, LITAF, DAPK2, SMAD3, RAF1, SULF1, NF1, TGFA, SHH, SOX9, CDH1	RAF1, SULF1, CDC27, KRAS, SHH, SOX9, TGFA, SMAD3, CCR2, NF1, ETS1, NCOR2, TAF6, CIAO1, DOCK2, TGFBR3
miR-301a-3p	EDN1, PTEN, MET, UCP3, CDKN1A, USP28	EDA, PTGES3	ROBO2, SOS1, USP47, DEDD, TRIM2, MDM4, SRA1, TGFA, PTEN, EDN1, USP28, SULF1, ROBO1, RUNX3, IRF1, E2F2, ROCK1, CDK5R1, CDKN1A, HIPK3, SIK1, PAK6, SOS2	EDN1, PTEN, CDKN1A, MET, E3F7, BMPR2, WNT2B, LIPA, CSF1, ZEB2, HPRT1, HHEK1, SRA1, CDK5R1, TGFA, IRF1, IL15, LRP2, USP28, SULF1, ROBO1, RUNX3, MDM4, MXD1, EREG, BHLHE41
miR-3607-5p	SIRT1, TIMP3, EDNRA, UCP3, ITGAV	−	SGK1, FOXA1, TIAM1, PEG3, EDNRA, SIRT1, CUL3, SKP2, REST, NRG1, APAF1, ATG5, FOXO3, GAS6, IRS2, BMI1, MCL1, NOTCH1, SOS1	SGK1, CDC27, FBXW7, NDN, EDNRA, SIRT1, CUL3, SKP2, NRG1, FOXO3, GAS6, IRS2, E2F4, MAGI2, BMI1, PRG4, NOTCH1, REST, TGFBR3, EVI5, PBX1, TOB1, BLM
miR-28-5p	−	APC, CDSN	APC, STK4, DDX5, CNTFR, BAG1, WNK3, NF1, PAK2	CNTFR, STK4, HTR4, CDK10, APC, NF1, TNS3, TRIM27
miR-9-5p	PTEN, NPM1, SIRT1, NOX4, ZNF354A	ASCL4	BCL6, EDAR, SIK1, PDCD6IP, REST, MEF2C, HIPK1, TCF7, PTEN, NPM1, SIRT1, FGF10, AR, BAG4, MAPK3K1	NOX4, LRRK2, FGF10, REST, PTEN, NPM1, SIRT1, SHC1, BCL6, CDK13, HES1, LIFR, MEF2C, HIPK1, AR, TCF7, DRD2, NRSA2, ODZ1, ID4
miR-33a-5p	MAPK14, CDK6, MME	−	SAV1, HIPK2, GPAM, CLCF1, MAPK14, GAS1, PSMD1, CREB1, ING3, SIX4	CLCF1, GAS1, DISC1, CASK, CDK6, SAV1, HIPK2, GPAM, EIF5A2, INSL4

Table S3. Continued.

miRNA (*Homo sapiens*)	Target genes and functions			
	Aging	Skin development	Apoptosis	Cell proliferation
miR-152	MNT, PTEN, RTN4, LRP2, IL15, UCP3	APC	MNT, PTEN, RTN4, PPARG, APC, CDKN1B, TGFA, MITF, MDM4, IGF1, GRID2, MAX, HIPK3, COL2A1, USP7	MDM4, IGF1, CDK13, EMX2, MNT, PTEN, LRP2, APC, ADAM10, CSF1, MAFG, CDKN1B, TGFA, MITF, CDC14A, E2F7
miR-19b-1-5p	HMGA2, MME	BCL11B	HMGA2, BCL11B, NAIP, CREB1, TRIM2, DSG3	HMGA2, BCL11B, GLMN, PBX1, EVI5, SLAMF1
let-7a-3p	TGFBR1, ID2, VCAM1, TFRC	TCF7L2, JUP	SNAI1, TGFBR1, SOX9, SMO, MECOM, CUL1, JAG2, SGK3, RAD21, CREB1, ID1, ROCK1, JAX2, CUL5, SNAI1, GSK3B, MEF2C, MALT1, FOXO1, ECT2, USP7	JAG2, MEF2C, SGK3, MALT1, TCF7L2, AHR, FOXO1, JAX2, SOX9, SMO, MECOM, CUL1, CUL5, LIPG, ID2, PELI1, ID4, SNAI1, TGFBR1, VCAM1, PAX6, TOB1
miR-431-3p	–	–	–	–
miR-625-3p	HMGA2	–	HMGA2, USP47, WNK3	HMGA2, KLF5, PURA

Table S4. Main functions of top 15 upregulated miRNAs, as predicted by bioinformatic analysis.

miRNA (*Homo sapiens*)	Putative target genes	KEGG pathway	Genes involved in the term	% of involved genes/ total genes	*P*-value
miR-1471	–	–	–	–	0.00E+00
miR-548q	178	Progesterone-mediated oocyte maturation	5	2.8	4.00E-03
		Axon guidance	4	2.2	7.50E-02
		Long-term potentiation	3	1.7	9.50E-02
miR-135a-3p	140	–	–	–	–
miR-134	245	Chemokine signaling pathway	7	2.9	1.70E-02
		Cytokine-cytokine receptor interaction	7	2.9	7.10E-02
		Jak-STAT signaling pathway	6	2.4	2.90E-02
		Calcium signaling pathway	6	2.4	4.60E-02
		Focal adhesion	6	2.4	7.30E-02
		Regulation of actin cytoskeleton	6	2.4	9.20E-02
		B cell receptor signaling pathway	5	2	9.60E-03
		T cell receptor signaling pathway	5	2	3.20E-02
		Acute myeloid leukemia	4	1.6	2.70E-02
		Chronic myeloid leukemia	4	1.6	5.10E-02
		ECM-receptor interaction	4	1.6	6.70E-02
		Prostate cancer	4	1.6	7.70E-02
		Dilated cardiomyopathy	4	1.6	8.30E-02
		Melanogenesis	4	1.6	9.90E-02
miR-4327	112	Long-term potentiation	3	2.7	3.70E-02
		Melanoma	3	2.7	4.00E-02
		Progesterone-mediated oocyte maturation	3	2.7	5.70E-02
		Oocyte meiosis	3	2.7	8.70E-02
miR-3137	285	Cell cycle	8	3	1.10E-03
miR-1181	2	–	–	–	–
miR-718	10	–	–	–	–
miR-622	210	Wnt signaling pathway	5	2.4	7.90E-02
		Prostate cancer	4	1.9	7.10E-02
miR-345-5p	94	Axon guidance	3	3.2	8.20E-02
		Natural killer cell mediated cytotoxicity	3	3.2	8.70E-02
miR-1273c	12	–	–	–	–
miR-1224-5p	213	Axon guidance	4	1.9	1.00E-01
miR-3945	68	Neurotrophin signaling pathway	3	4.4	8.40E-02
		Ubiquitin mediated proteolysis	3	4.4	1.00E-01
miR-3188	222	Tight junction	6	2.7	2.60E-02
miR-1306-3p	12	–	–	–	–

Table S5. Main functions of top 15 downregulated miRNAs, as predicted by bioinformatic analysis.

miRNA (*Homo sapiens*)	Putative target genes	KEGG pathway	Genes involved in the term	% of involved genes/ total genes	*P*-value
miR-221-5p	159	–	–	–	–
miR-29b-1-5p	256	Insulin signaling pathway	5	1.9	8.50E-02
miR-140-5p	234	Regulation of actin cytoskeleton	7	3	5.90E-02
miR-7-1-3p	891	Pathways in cancer	32	3.6	3.70E-05
		Wnt signaling pathway	22	2.5	2.30E-06
		MAPK signaling pathway	20	2.2	2.60E-02
		Ubiquitin mediated proteolysis	15	1.7	2.70E-03
		ErbB signaling pathway	11	1.2	4.70E-03
		Cell cycle	11	1.2	4.90E-02
		Insulin signaling pathway	11	1.2	7.50E-02
		TGF-beta signaling pathway	10	1.1	1.40E-02
miR-493-3p	273	Pathways in cancer	11	4	2.50E-02
		Chemokine signaling pathway	9	3.3	6.90E-03
		MAPK signaling pathway	9	3.3	4.80E-02
		Melanogenesis	7	2.6	3.60E-03
		GnRH signaling pathway	6	2.2	1.60E-02
miR-301a-3p	470	Regulation of actin cytoskeleton	13	2.8	1.30E-02
		Cytokine-cytokine receptor interaction	13	2.8	4.90E-02
		Insulin signaling pathway	10	2.1	1.00E-02
		TGF-beta signaling pathway	9	1.9	2.20E-03
		Phosphatidylinositol signaling system	8	1.7	3.50E-03
		ErbB signaling pathway	7	1.5	2.90E-02
		p53 signaling pathway	6	1.3	3.50E-02
		mTOR signaling pathway	5	1.1	5.00E-02
		Inositol phosphate metabolism	5	1.1	5.70E-02
miR-3607-3p	458	Axon guidance	11	2.4	7.40E-04
		Ubiquitin mediated proteolysis	10	2.2	4.30E-03
		Wnt signaling pathway	8	1.7	6.00E-02
		Cell cycle	7	1.5	6.90E-02
		Gap junction	6	1.3	5.50E-02
miR-28-5p	157	MAPK signaling pathway	7	4.5	1.20E-02
		Axon guidance	4	2.5	6.60E-02
miR-9-5p	610	MAPK signaling pathway	18	3	4.60E-03
		Pathways in cancer	18	3	3.10E-02
		Neurotrophin signaling pathway	11	1.8	5.80E-03
		Jak-STAT signaling pathway	11	1.8	2.50E-02
		Chemokine signaling pathway	11	1.8	7.40E-02
miR-33a-5p	264	Axon guidance	7	2.7	6.20E-03
miR-152	459	Pathways in cancer	18	3.9	3.30E-03
		Insulin signaling pathway	8	1.7	5.30E-02
		ECM-receptor interaction	7	1.5	1.90E-02
		ErbB signaling pathway	7	1.5	2.20E-02
		TGF-beta signaling pathway	7	1.5	2.20E-02
		Cell cycle	7	1.5	9.40E-02
		p53 signaling pathway	6	1.3	2.80E-02
miR-19b-1-5p	133	Calcium signaling pathway	6	4.5	2.40E-03
		Huntington's disease	5	3.8	1.60E-02
		Insulin signaling pathway	4	3	3.70E-02
		Alzheimer's disease	4	3	5.90E-02
let-7a-3p	438	Pathways in cancer	15	3.4	2.60E-02
		Endocytosis	11	2.5	1.30E-02
		Regulation of actin cytoskeleton	11	2.5	3.40E-02
		TGF-beta signaling pathway	9	2.1	1.10E-03
		Chemokine signaling pathway	9	2.1	8.20E-02
		Adherens junction	8	1.8	2.40E-03
		Wnt signaling pathway	8	1.8	7.20E-02
miR-431-3p	3	–	–	–	–
miR-625-3p	80	Neurotrophin signaling pathway	3	3.8	7.00E-02

SY Kim, JH Son, HJ Han, S Li, SY Kim, and I-S An performed experiments and analyzed the data. KJ Ahn, S An, and S Bae conceived and designed the study. HJ Cha, S An, and S Bae prepared the manuscript. S Bae was responsible for the overall project. All authors discussed the results and approved the final version of manuscript.

Conflict of Interest The authors state no conflict of interest.

References

1. Lawrence, N. S., Beckett, E. L., Davis, J. & Comptonm, R.G. Voltammetric investigation of hair dye constituents: application to the quantification of *p*-phenylenediamine. *Analyst* **126**:1897-900 (2001).
2. Corbett, J. F. An historical review of the use of dye precursors in the formulation of commercial oxidation hair dyes. *Dyes Pigments* **41**:127-136 (1999).
3. Brown, K. C. in Hair and Hair Care (eds Johnson, D.) 191-215 (Marcel Dekker, New York, 1997).
4. Gendler, E. Adverse reaction to cosmetics. *Cutis* **39**: 525-526 (1987).
5. Moeller, R., Lichter, J. & Blömeke, B. Impact of paraphenylenediamine on cyclooxygenases expression and prostaglandin formation in human immortalized keratinocytes (HaCaT). *Toxicology* **249**:167-175 (2008).
6. Eilstein, J., Giménez-Arnau, E., Duché, D., Rousset, F. & Lepoittevin, J. P. Mechanistic studies on the lysine-induced N-formylation of 2,5-dimethyl-p-benzoquinonediimine. *Chem Res Toxicol* **20**:1155-1161 (2007).
7. McFadden, J. P., Yeo, L. & White, J. L. Clinical and experimental aspects of allergic contact dermatitis to para-phenylenediamine. *Clin Dermatol* **29**:316-324 (2011).
8. So, J. Y., Shin, C. Y., Song, M., Rha, Y. A. & Ryu, J. C. Gene expression profiling of hair-dying agent, paraphenylenediamine, in human keratinocytes (HaCaT) cells. *Mol Cell Toxicol* **7**:339-346 (2011).
9. Moeller, R., Lichter, J. & Blömeke, B. Impact of paraphenylenediamine on cyclooxygenases expression and prostaglandin formation in human immortalized keratinocytes (HaCaT). *Toxicology* **249**:167-175 (2008).
10. Chung, K. T. *et al*. Mutagenicity and toxicity studies of p-phenylenediamine and its derivatives. *Toxicol Lett* **81**:23-32 (1995).
11. Chye, S. M. *et al*. Apoptosis induced by para-phenylenediamine involves formation of ROS and activation of p38 and JNK in chang liver cells. *Environ Toxicol* **29**:981-990 (2014).
12. Sontheimer, E. J. & Carthew, R. W. Silence from within: endogenous siRNAs and miRNAs. *Cell* **122**:9-12 (2005).
13. Hooff, G. P. *et al*. Analytical Investigations of Toxic p-Phenylenediamine (PPD) Levels in Clinical Urine Samples with Special Focus on MALDI-MS/MS. *PLoS One* **6**:e22191 (2011).
14. Tsutsumi, S. *et al*. Gastric irritant-induced apoptosis in guinea pig gastric mucosal cells in primary culture. *Biochim Biophys Acta* **1589**:168-180 (2002).
15. Nakai, K., Yoneda, K. & Kubota, Y. Oxidative stress in allergic and irritant dermatitis: from basic research to clinical management. *Recent Pat Inflamm Allergy Drug Discov* **6**:202-209 (2012).
16. Jovanovic, M. & Hengartner, M. O. miRNAs and apoptosis: RNAs to die for. *Oncogene* **25**:6176-6187, (2006).
17. Bueno, M. J. & Malumbres, M. MicroRNAs and the cell cycle. *Biochim Biophys Acta* **1812**: 592-601 (2011).
18. Xu, S. *et al*. Oxidative stress mediated-alterations of the microRNA expression profile in mouse hippocampal neurons. *Int J Mol Sci* **13**:16945-16960 (2012).
19. Cui, L. *et al*. MicroRNA-99a induces G1-phase cell cycle arrest and suppresses tumorigenicity in renal cell carcinoma. *BMC Cancer* **12**:546 (2012).
20. Liu, Q. *et al*. miR-16 family induces cell cycle arrest by regulating multiple cell cycle genes. *Nucleic Acids Res* **36**:5391-5404 (2008).
21. Cimmino, A. *et al*. miR-15 and miR-16 induce apoptosis by targeting BCL2. *Proc Natl Acad Sci U S A* **102**:13944-13949 (2005).
22. Zhang, X. *et al*. MicroRNA-21 modulates the levels of reactive oxygen species levels by targeting SOD3 and TNFα. *Cancer Res* **72**:4707-4713 (2012).
23. An, Y. R. & Hwang, S. Y. Toxicology study with microRNA. *Mol Cell Toxicol* **10**:127-134 (2014).
24. Lema, C. & Cunningham, M. J. MicroRNAs and their implications in toxicological research. *Toxicol Lett* **5**:100-105 (2010).
25. Chen, S. C. *et al*. *p*-Phenylenediamine induces p.53-mediated apoptosis in Mardin Darby canine Kidney cells. *Toxicol In Vitro* **20**:801-807 (2006).
26. Chen, S. C. *et al*. Para-phenylenediamine induced DNA damage and apoptosis through oxidative stress and enhanced caspase-8 and -9 activities in Mardin-Darby canine kidney cells. *Toxicol In Vitro* **24**:1197-1202 (2010).
27. Ohdaira, H., Sekiguchi, M., Miyata, K. & Yoshida, K. MicroRNA-494 suppresses cell proliferation and induces senescence in A549 lung cancer cells. *Cell Prolif* **45**:32-38 (2012).
28. Romano, G. *et al*. MiR-494 is regulated by ERK1/2 and modulates TRAIL-induced apoptosis in non-small-cell lung cancer through BIM down-regulation. *Proc Natl Acad Sci U S A* **109**:16570-16575 (2012).
29. Saini, S. *et al*. MicroRNA-708 induces apoptosis and suppresses tumorigenicity in renal cancer cells. *Cancer Res* **71**:6208-6219 (2011).
30. Wada, T. & Penninger, J. M. Mitogen-activated protein kinases in apoptosis regulation. Oncogene **23**: 2838-2849 (2004).
31. Zhang, W. & Liu, H. T. MAPK signal pathways in the regulation of cell proliferation in mammalian cells. *Cell Res* **12**:9-18 (2002).